Randomly Oriented ZnO Nanorods As Advanced Substrate for High-Performance Protein Microarrays

Weihua Hu, Yingshuai Liu, Zhihong Zhu, Hongbin Yang, and Chang Ming Li*

School of Chemical and Biomedical Engineering, Centre for Advanced Bionanosystems, Nanyang Technological University, 70 Nanyang Drive, Singapore 637457

ABSTRACT When aligned or patterned nanostructures attract great interest, the randomly arranged nanostructures are often ignored. A nanostructure with randomly oriented ZnO nanorods was prepared on the glass slides using scalable method as a protein microarray substrate. It demonstrates significant fluorescence enhancement and superior performance over the aligned ZnO nanorods for high performance protein microarray applications.

KEYWORDS: ZnO nanorods • fluorescence enhancement • protein microarray • random orientation

With the completion of the human genome project, the high-throughput protein microarray has become more important in life science (1−4). Fluorescence is the predominant detection technique for microarrays, but it remains a great challenge to sensitively detect low-abundance proteins, which is particularly critical in early diagnosis of various infectious diseases. A number of metal nanostructures known as "nanoantennas", can significantly enhance the emission intensity of proximal fluorophores as large as 50 folders (5−7), but the high cost of these materials limits their practical applications. Interestingly, ZnO nanorod, an economic material shows the similar capability to improve the fluorescence intensity, regardless of the spectral characteristic of fluorophores in close proximity (8−12). However, all the previous works on the ZnO nanorods for fluorescence enhancement are demonstrated by using only prepatterned nanostructures, which limits the detection capacity and, most importantly, requires expensive microfabrication techniques, and is difficult for large-scale production (8−12). Until now, no reported work uses ZnO nanorods as a high performance substrate to fabricate protein microarrays by the robot chip writer, although a wide variety of ZnO nanostructures have been successfully synthesized by either solution growth or vapor deposition (13−15).

To utilize the strong fluorescence-amplifying capability of ZnO nanorods for high-throughput microarray application while eliminaing the expensive pattern process, we prepared aligned and randomly oriented ZnO nanorods on glass slides with mass production methods, respectively. Using cyanine 3 (Cy3)-labeled anti-goat IgG as the model protein, protein microarrays were printed on these ZnO surfaces with a robot chip writer (BioRad, VersArray chip writer contact system) to examine their merits as advanced microarray substrates.

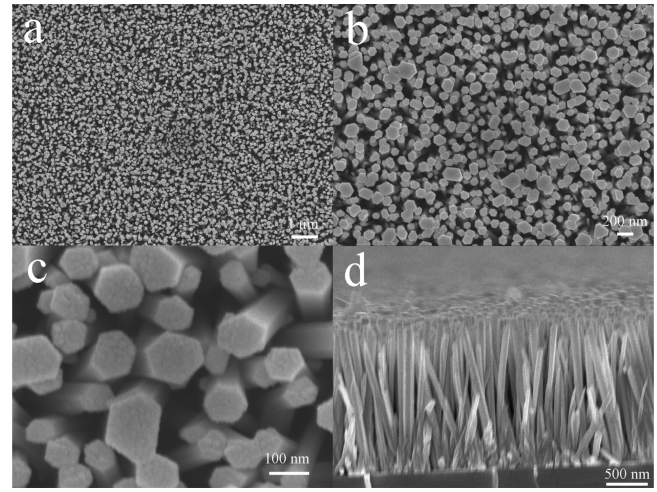

FIGURE 1. SEM images of aligned ZnO nanorods grown on glass. (a−c) top-view; (d) cross-section view

Zinc nitrate and ammonium hydroxide were used as the zinc source and complexing reagent, respectively to synthesize the ZnO nanorods by the conventional solution growth route (16, 17). The aligned ZnO nanorods with homogeneous distribution were grown from the precoated textured ZnO seeds (16). The scanning electron microscope (SEM) images of the nanorods in Figure 1 show a hexagonal structure with an average length and diameter of 1.3 μm and 100 nm, respectively. Growing from the textured ZnO seeds along the *c*-axis, the nanorods are vertical to the glass with their (0001) planes parallel to the substrate, which is further conformed by the predominant peak at 34.5° corresponding to (002) facet on the X-ray diffraction (XRD) pattern (Figure 2a).

Randomly oriented nanorods were synthesized on the permanganate-activated glass (17). Figure 3a depicts the SEM image of 1 h-grown ZnO nanorods, clearly showing

* Corresponding author. Fax: +65 6791 1761. Tel: +65 6790 4485. E-mail: ecmli@ntu.edu.sg.
Received for review April 8, 2010 and accepted May 25, 2010

DOI: 10.1021/am100314w

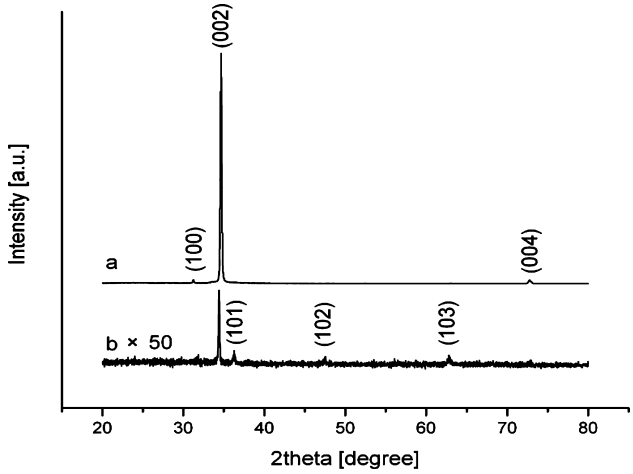

FIGURE 2. XRD patterns of aligned (a) ZnO nanorods and (b) random ZnO nanorods on glass.

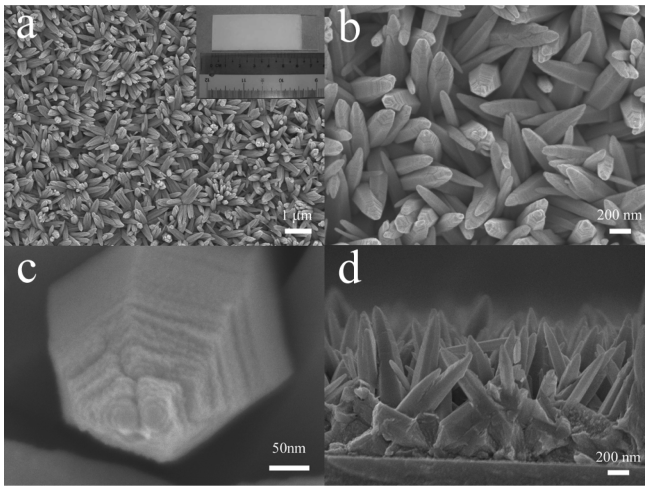

FIGURE 3. SEM images of randomly oriented ZnO nanorods grown on glass. (a–c) top-view; (d) Cross-section view

randomly oriented nanorods with uniform distribution on the glass. Actually, the whole slide surface (75 cm × 25 cm) is completely covered by a homogeneous thin gray-azury layer of the nanorods (inset of Figure 3a). The high-magnification image (Figure 3b) exhibits sharp tips of nanorods. The diameters of nanorods vary from 100 to 200 nm. The high resolution image of the tips in Figure 3c shows a hexagonal structure. The sharp tip is formed by the stack of a serial of hexagonal islands with gradually decreased diameters. The cross-section image in Figure 3d displays that the nanorods with average length of 1 μm anchored on a 300 nm amorphous layer on the glass. On the corresponding XRD pattern (Figure 2b), the peaks assigned to (101), (102), and (103) facets appear besides the (002) peak, suggesting the nanorods rest at all angles on the substrate. Compared with the aligned ZnO nanorod (Figure 2a), this pattern further proves its random orientation.

The growth process of the random nanorods was investigated by SEM, showing that some granular ZnO clusters with ca. 200 nm dimension composed of 20–30 nm nanoparticles are deposited on the surface after 10 min growth (see Figure S1 in the Supporting Information). The thickness of the cluster layer is ca. 300 nm according to the cross-section image. After 20 min growth, the clusters develop to initial nanorods with random directions, while the thickness increases to more than 500 nm (Figure S2 in the Supporting Information). On the XRD pattern (Figure S3), only a weak (002) peak appears at 34.5° for 10 min growth, indicating the polycrystalline nature of the ZnO thin film. With an extended growth time of 20 min, the peak intensity obviously rises because of the nanorod growth along the preferential *c*-axis direction. The SEM and XRD results elucidate a possible two-step growth mechanism: first formation of polycrystalline ZnO thin film on the surface, followed by the growth of ZnO nanorods from the thin layer along the *c*-axis direction to produce highly crystalline ZnO nanorods. The first heterogeneous nucleation step is ultimately crucial for the successful growth of ZnO nanorods, where the permanganate treatment of glass plays an important role. The nanorods can be grown reproducibly only when the glass was pretreated by permanganate. Otherwise, it is very hard to obtain tethered ZnO nanorods. In most cases, the deposits are sparse ZnO nanoflowers or scattered ZnO nanorods on the nonactivated glass (see Figure S4 in the Supporting Information). It is believed that absorbed manganese hydrated oxides (e.g., MnOOH, produced by permanganate reduction) act as nucleation centers for ZnO growth (17, 18). The activation method is universal regardless of substrates, enabling reliable synthesis of ZnO nanorods on various surfaces. In our laboratory, the random ZnO nanorods have been successfully grown on various substrates including some polymer surfaces.

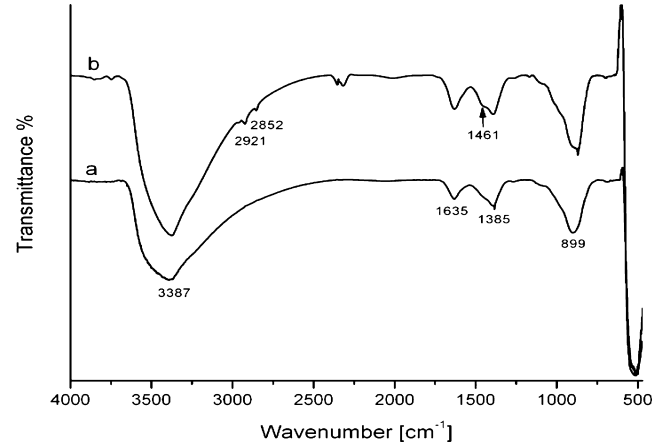

FIGURE 4. FTIR spectra of (a) pristine ZnO nanorods and (b) GPTS-modified nanorods.

For the protein attachment, the ZnO nanorods were functionalized by (3-glycidoxypropyl)trimethoxy silane (GPTS), of which the trimethoxy silane group reacted with ZnO to form Si–O–Zn bond (19, 20), whereas the epoxy group could be used to covalently bind to the amine groups of the protein (2). The binding between GPTS and ZnO is proved by the Fourier transform infrared (FTIR) spectroscopy (Figure 4). On the pristine nanorods, the broad peaks located at 3387 and 1635 cm^{-1} originate from the O–H stretching and bending vibrations of trace water on the nanorods. The strong adsorption at 500 cm^{-1} could be assigned to the stretching vibration of Zn–O bond. The incorporation of

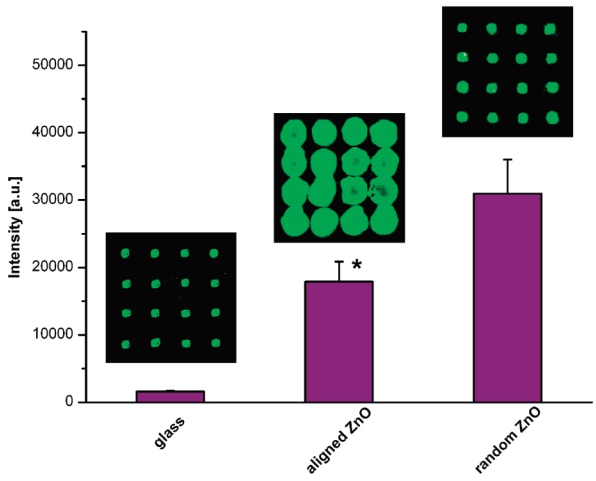

FIGURE 5. Fluorescence images and corresponding fluorescence intensities of Cy-3 conjugated anti-goat IgG 4 × 4 microarray fabricated on glass, aligned nanorods, and random nanorods. *Because of the irregular spot shape, the average intensity on aligned ZnO was collected from the biggest circle area on each spot.

carbonate species leads to the peaks at 1385 and 899 cm^{-1} (21). After modification, three peaks arise at 2921, 2852, and 1461 cm^{-1} due to the presence of methylene, implying the successful modification of ZnO.

Four × four microarrays of Cy-3-labeled anti-goat IgG were written onto the GPTS-modified aligned and random ZnO nanorods respectively by using the robotic spotter. For comparison, GPTS-modified glass was used as a substrate for the baseline. The representative fluorescence images and the corresponding fluorescence intensities of the microarrays are shown in Figure 5. The GPTS-modified glass exhibits good spot morphology (average diameter of 126 ± 5 μm), fluorescence homogeneity, and low spot-to-spot deviation (intensity of 1564 ± 128 au). The aligned ZnO nanorods enhance the fluorescence more than 1 order of magnitude (17877 ± 2967 au) in comparison to the plain glass, indicating the strong fluorescence enhancement effect of ZnO nanorods. However, the spots have very large diameters and irregular shapes, and some neighboring spots merge together. Even in each spot the intensity is nonuniform with a ring pattern, which cannot be suppressed by adding an appropriate surfactant (Triton X100) in the printing buffer as the reported works (22). The poor homogeneity and morphology of the spots are very likely to originate from a strong capillary effect in the nanochannels between the aligned nanorods, resulting in irregular expansion and disorder transport of the spotted protein solution. The microarray printed on the aligned ZnO nanorods has significant intensity variation and thus is difficult to have practical applications, although it can enhance the fluorescence greatly. Surprisingly, the microarray on the random ZnO nanorods shows good morphology and homogeneity with average diameter of 153 ± 8 μm. This is possibly attributed to the random orientation, low population density, and low length/diameter ratio of the ZnO nanorods prepared, which can significantly reduce the capillary effect. Importantly, in comparison to the glass and oriented ZnO nanorods, the random nanorods demonstrate the highest fluorescence intensity of 30962 ± 5041 au, a nearly 20-fold of that on glass and 70% higher than that of aligned ZnO nanorods even though its population density of nanorods is obviously lower than that of aligned ZnO nanorods (ca. 20 vs 100 per μm^2 according to the SEM images). In addition, the random structure is also much superior to the aligned ZnO nanorods in terms of intensity homogeneity, which is very critical parameter in microarray application. The ZnO thin film (see Figure S1 in the Supporting Information) also displays fluorescence enhancement (9602 ± 571 au, see Figure S5 in the Supporting Information), although much weaker than the random nanorods, indicating that other ZnO nanostructures possess the intrinsic fluorescent enhancement effect.

To find out why the random nanorods have higher fluorescence intensity than the aligned ones, microarrays of alkaline phosphatase (ALP)-conjugated anti-goat IgG were fabricated and the attached protein was quantified by electrochemical method in the substrate (*p*-aminophenyl phosphate, PAPP) solution (see details in the Supporting Information) (23, 24). It is found that the surface densities of attached proteins on glass, aligned nanorods, and random nanorods have an approximate ratio of 1:1.9:2.9. It can be easily understood that the protein density on aligned nanorods is higher than that on the glass. Notably, the random nanorods display highest protein loading density even than the aligned ones. It is very possible that the surface area of the random ZnO nanorods could be used much more efficiently than the aligned ones. From Figure 5, the fluorescence enhancement factors of the random ZnO nanorods to the aligned ones and plain glass slide is found to be 1.7 and 19.8, respectively. Apparently, the enhancement not only comes from the ZnO intrinsic fluorescent enhancement effect, but also the high surface protein loading capacity caused by its random structure.

Taking into account the good spot morphology and intensity homogeneity together with the high signal-amplifying ability, the randomly oriented ZnO nanorods are undoubtedly an excellent candidate as a fluorescence-enhancing substrate for protein microarrays. The application of this platform for sensitive detection of specific biomarkers is currently ongoing in our laboratory and will be published separately.

In summary, the orientation of ZnO nanorods has an essential effect on their microarray applications. Compared with the aligned nanorods, the randomly oriented ones show advantageous performance in terms of spot morphology, intensity homogeneity, and protein loading density because the capillary effect is effectively eliminated under the random configuration. At the same time, the synthesis procedure is much easier for mass production, and the as-prepared randomly oriented nanorods are compatible with the mature microarray fabrication technique, offering the attractive prospect for low-cost and high-performance microarray applications.

Acknowledgment. We acknowledge the financial support from the Center for Advanced Bionanosystems, Nanyang Technological University.

Supporting Information Available: Description of experimental details, additional SEM images, XRD patterns, and electrochemical quantification of attached proteins on three substrates (PDF). This materials is available free of charge via the Internet at http://pubs.acs.org.

REFERENCES AND NOTES

(1) Yu, L.; Liu, Y. S.; Gan, Y.; Li, C. M. *Biosens. Bioelectron.* **2009**, *24*, 2997–3002.
(2) Liu, Y. S.; Li, C. M.; Hu, W. H.; Lu, Z. S. *Talanta* **2009**, *77*, 1165–1171.
(3) Liu, Y. S.; Li, C. M.; Yu, L.; Chen, P. *Front. Biosci.* **2007**, *12*, 3768–3773.
(4) Liu, Y.; Hu, W.; Lu, Z.; L, C. M. *MedChemComm* **2010**; DOI: 10.1039/c0md00032a.
(5) Kuhn, S.; Hakanson, U.; Rogobete, L.; Sandoghdar, V. *Phys. Rev. Lett.* **2006**, *97*.
(6) Cheng, D. M.; Xu, Q. H. *Chem. Commun.* **2007**, 248–250.
(7) Staiano, M.; Matveeva, E. G.; Rossi, M.; Crescenzo, R.; Gryczynski, Z.; Gryczynski, I.; Iozzino, L.; Akopova, I.; D'Auria, S. *ACS Appl. Mater. Interfaces* **2009**, *1*, 2909–2916.
(8) Dorfman, A.; Kumar, N.; Hahm, J. *Adv. Mater.* **2006**, *18*, 2685-+.
(9) Dorfman, A.; Kumar, N.; Hahm, J. I. *Langmuir* **2006**, *22*, 4890–4895.
(10) Zhao, J. W.; Wu, L. Z.; Zhi, J. F. *J. Mater. Chem.* **2008**, *18*, 2459–2465.
(11) Adalsteinsson, V.; Parajuli, O.; Kepics, S.; Gupta, A.; Reeves, W. B.; Hahm, J. I. *Anal. Chem.* **2008**, *80*, 6594–6601.
(12) Kumar, N.; Dorfman, A.; Hahm, J. *Nanotechnology* **2006**, *17*, 2875–2881.
(13) Wang, Z. L. *J. Phys.: Condens. Matter* **2004**, *16*, R829–R858.
(14) Hwang, J. K.; Cho, S.; Seo, E. K.; Myoung, J. M.; Sung, M. M. *ACS Appl. Mater. Interfaces* **2009**, *1*, 2843–2847.
(15) Wang, X. L.; Yang, F.; Yang, W.; Yang, X. R. *Chem. Commun.* **2007**, 4419–4421.
(16) Greene, L. E.; Law, M.; Tan, D. H.; Montano, M.; Goldberger, J.; Somorjai, G.; Yang, P. D. *Nano Lett.* **2005**, *5*, 1231–1236.
(17) Kokotov, M.; Hodes, G. *J. Mater. Chem.* **2009**, *19*, 3847–3854.
(18) Kokotov, M.; Biller, A.; Hodes, G. *Chem. Mater.* **2008**, *20*, 4542–4544.
(19) Taratula, O.; Galoppini, E.; Wang, D.; Chu, D.; Zhang, Z.; Chen, H. H.; Saraf, G.; Lu, Y. C. *J. Phys. Chem. B* **2006**, *110*, 6506–6515.
(20) Yu, H.-h.; Wong, M. K. F.; Ali, E. M.; Ying, J. Y. *Chem. Commun.* **2008**, 4912–4914.
(21) Mustafa, S.; Shahida, P.; Naeem, A.; Dilara, B.; Rehana, N. *Langmuir* **2002**, *18*, 2254–2259.
(22) Deng, Y.; Zhu, X. Y.; Kienlen, T.; Guo, A. *J. Am. Chem. Soc.* **2006**, *128*, 2768–2769.
(23) Dong, H.; Li, C. M.; Chen, W.; Zhou, Q.; Zeng, Z. X.; Luong, J. H. T. *Anal. Chem.* **2006**, *78*, 7424–7431.
(24) Dong, H.; Li, C. M.; Zhou, Q.; Sun, J. B.; Miao, J. M. *Biosens. Bioelectron.* **2006**, *22*, 621–626.

AM100314W